Available online at www.sciencedirect.com
ScienceDirect
Journal of Power Sources 167 (2007) 39–46
JOURNAL OF POWER SOURCES
www.elsevier.com/locate/jpowsour

Performance of $La_{0.75}Sr_{0.25}Cr_{0.5}Mn_{0.5}O_{3-\delta}$ perovskite-structure anode material at lanthanum gallate electrolyte for IT-SOFC running on ethanol fuel

Bo Huang *, S.R. Wang, R.Z. Liu, X.F. Ye, H.W. Nie, X.F. Sun, T.L. Wen

Shanghai Institute of Ceramics, Chinese Academy of Sciences (SICCAS), 1295 Dingxi Road, Shanghai 200050, PR China

Received 1 February 2007; accepted 8 February 2007
Available online 22 February 2007

Abstract

Perovskite-structure $La_{0.75}Sr_{0.25}Cr_{0.5}Mn_{0.5}O_{3-\delta}$ (LSCM) powders were prepared using a simple combustion process. Thermal analysis was carried out on the perovskite precursor to investigate the oxide-phase formation. The structural phase of the powders was determined by X-ray diffraction. These results showed that the decomposition of the precursors occurs in a two-step reaction and temperatures higher than 1100 °C are required for these decomposition reactions. For the electrochemical characterization, LSCM anode materials and $(Pr_{0.7}Ca_{0.3})_{0.9}MnO_3$ (PCM) cathode materials were screen-printed on two sides of dense $La_{0.8}Sr_{0.2}Ga_{0.8}Mg_{0.2}O_3$ (LSGM) electrolyte layers prepared by tape casting with a thickness of about 600 μm, respectively. The morphology of the screen-printed $La_{0.75}Sr_{0.25}Cr_{0.5}Mn_{0.5}O_{3-\delta}$ perovskite thick films (65 μm) was investigated by field emission scanning electron microscope and showed a porous microstructure. In addition, fuel cell tests were carried out using humidified hydrogen or ethanol stream as fuel and oxygen as oxidant. The performance of the conventional electrolyte-supported cell LSCM/LSGM/PCM while operating on humidified hydrogen was modest with a maximum power density of 165, 99 and 62 mW cm^{-2} at 850, 800 and 750 °C, respectively, the corresponding values for the cell while operating on ethanol stream was 160, 101 and 58 mW cm^{-2}, respectively. Cell stability tests indicate no significant degradation in performance has been observed after 60 h of cell testing when LSCM anode was exposed to ethanol steam at 750 °C, suggesting that carbon deposition was limited during cell operation.

Keywords: Anode; Carbon deposition; Electrochemical impedance spectroscopy; Ethanol; LSGM; Solid oxide fuel cell (SOFC)

1. Introduction

Solid oxide fuel cell (SOFC) is an all solid device that converts the chemical energy of gaseous such as hydrogen and natural gas to electricity through electrochemical processes. SOFC, being an electrochemical device, has unique advantages over the traditional power generation technologies. SOFCs combine the benefits of environmentally benign power generation with fuel flexibility. For many applications such as combined cycle with gas turbines and heat cogeneration, the high SOFC temperatures up to 1000 °C offer significant advantages. These high temperatures present significant problems for materials selection and durability, especially for smaller scale applications; thus, there is also considerable impetus to develop lower temperature SOFC systems. A decrease in the operation temperature means a loss of power density mainly due to a considerable reduction of both ionic conductivity of the electrolyte and catalytic activity of the electrodes. To avoid ohmic loss, the thickness of the electrolyte might be reduced or alternative electrolyte materials used, providing that they offer good performance for operation at intermediate temperatures (≤800 °C). For example, it is necessary to reduce the thickness of yttrium-stabilized zirconia (YSZ) electrolyte to at least 15 μm to achieve comparable performances at 700 °C [1]. In addition, SOFCs require hydrogen as the fuel, but viable near-term applications will need to use the more readily available hydrocarbons, such as methane. Therefore, much effort has been devoted in developing reduced-temperature solid oxide fuel cells (SOFCs) running on hydrocarbon fuels instead of hydrogen [2–5]. However, conventional Ni-based anode suffers a number of drawbacks in systems where hydrocarbon fuel is used such as carbon deposition since Ni is a good catalyst for hydrocarbon cracking reaction. Carbon

* Corresponding author. Tel.: +86 21 52411520; fax: +86 21 52413903.
E-mail address: huangbo2k@hotmail.com (B. Huang).

0378-7753/$ – see front matter © 2007 Elsevier B.V. All rights reserved.
doi:10.1016/j.jpowsour.2007.02.022

deposition covers the active sites of the anode, resulting in rapid, irreversible cell deactivation [6–10].

Recently, perovskite $La_{1-x}Sr_xGa_{1-y}Mg_yO_{3-\delta}$ (LSGM) having oxygen vacancies attracts much attention for its high ionic conductivity at low temperature [11]. The oxygen ionic conductivity of LSGM at 800 °C was measured as 0.1 S cm^{-1}, which corresponded to that of YSZ at 1000 °C [12,13]. LSGM is one of the promising materials for SOFCs operating at ca. 800 °C [14,15].

Replacing Ni/YSZ cermet anodes by Ni-free oxide, such as ceria, titanate and lanthanum chromite-based oxides has attracted a great attention recently. Doped $LaCrO_3$-based materials have been extensively investigated as interconnect material in SOFC [16]. $LaCrO_3$-based oxide such as $(LaSr)CrO_3$ was shown to have very low activity towards carbon deposition [17]. Catalytic activity of $LaCrO_3$ for methane oxidation can also be substantially enhanced by partial substitution at A- and B-sites. Sfeir et al. [18,19] studied the thermodynamic stability and the catalytic activity of $(LaA)(CrB)O_3$ system (A = Ca, Sr and B = Mg, Mn, Fe, Co, Ni) as alternative anode materials under simulated SOFC operation conditions. Thermodynamically, Sr and Mn substitution maintains the stability of the perovskite while other substitutes destabilize the system. Recently, Tao and Irvine [20,21] reported promising results of $La_{0.75}Sr_{0.25}Cr_{0.5}Mn_{0.5}O_3$ (LSCM) as anode for SOFC. LSCM is a p-type conductor with conductivity of ∼38 S cm^{-1} in air and 1.5 S cm^{-1} in 5% H_2 at 900 °C. The electrode polarization resistance for the oxidation reactions in wet CH_4 and H_2 at 900 °C was 0.85 and 0.26 Ω cm^2, respectively. The performances are considered to be compatible to the Ni/YSZ cermet anodes.

In this work, LSGM was tested as electrolyte using $(Pr_{0.7}Ca_{0.3})_{0.9}MnO_3$ (PCM) and $La_{0.75}Sr_{0.25}Cr_{0.5}Mn_{0.5}O_{3-\delta}$ (LSCM) as cathode and anode, respectively. The fabrication and performance of electrolyte-supported system LSCM/LSGM/PCM were investigated to assess their feasibility as alternative anode material for ethanol oxidation reactions for SOFC.

2. Experimental

2.1. Synthesis of electrode and electrolyte

The composition of LSCM anode was chosen as $La_{0.75}Sr_{0.25}Cr_{0.5}Mn_{0.5}O_{3-\delta}$ (LSCM) [20,21]. $La_{0.75}Sr_{0.25}Cr_{0.5}Mn_{0.5}O_{3-\delta}$ anode material was prepared using a combustion synthesis technique. Stoichiometric amounts of lanthanum nitrate ($La(NO_3)_3{\cdot}6H_2O$), strontium nitrate ($Sr(NO_3)_2$), chromium nitrate ($Cr(NO_3)_3{\cdot}9H_2O$) and manganese nitrate ($Mn(NO_3)_2$) were dissolved in distilled water with constant stirring. Then, a stoichiometric amount of citric acid ($C_6H_8O_7{\cdot}H_2O$), which is a chelating agent and fuel, was also dissolved in this solution. The stoichiometric ratio of citric acid to nitrates was calculated according to Jain et al. [22]. The solution pH was adjusted to 7 with the addition of concentrated ammonia solution. A gel was formed with continuous stirring and mild heating (∼110 °C). The gel was dried at room temperature for over 12 h and then fired at 350 °C for 30 min. The resulting powders were ground in an agate mortar and fired in air at 1000 °C for 5 h, ground again and finally fired at 1200 °C for 5 h in air.

$La_{0.8}Sr_{0.2}Ga_{0.8}Mg_{0.2}O_3$ (LSGM) used as the electrolyte was prepared from stoichiometric amounts of La_2O_3 (>99.99% purity), $SrCO_3$ (>99.9% purity), Ga_2O_3 (>99.99% purity) and MgO (>99.99% purity) by traditional solid-state reaction method. Before weighing, La_2O_3 was heat-treated at 1000 °C for over 3 h in order to achieve decarbonation and dehydration. The powders were intimately mixed in an agate mortar with the aid of absolute alcohol for 24 h and then calcined at 950 °C for 10 h. The calcined powders were ground using agate mortar and pestle and ball-milled in absolute alcohol for another 24 h. The resulting fine powders were dried and uniaxially pressed into dense pellet (99% of theoretical density) and then sintered at 1500 °C for 6 h in air.

2.2. Preparation of LSGM electrolyte matrix

The procedure for obtaining LSGM electrolyte matrix by tape casting samples comprised the preparation of a slurry containing LSGM powder, azeotropic mixture of butanone and ethyl alcohol absolute as solvent. Triethanolamine as a kind of zwitterionic dispersant to reduce the interfacial tension between the surface of the particle and the liquid; polyethylene glycol (PEG 200) as plasticizer to increase the flexibility of the tapes; and poly-vinyl-butyl (PVB) as binder to provide their strength after the evaporation of the solvent. The PVB binder was supplied as a free flowing fine-grained powder and the PEG plasticizer was obtained in a liquid form. All the organic additives were supplied by Shanghai Chem. Ltd., China. Intermediate ball-milling steps are used for the preparation of the tapes. After the mixing and the homogenization of the slurry were completed, the slurry was degassed using a vacuum pump (pressure: 200 mbar absolute) and cast on a casting surface of polyethylene film by a "doctor-blade" method. The cast tapes were allowed to dry at room temperature for 48 h. After the solvent in the tapes was completely evaporated, the LSGM green tapes were obtained. They were then sintered in air at 1500 °C for 5 h. Thus, a disk-shaped electrolyte substrate, having a diameter of about 3.0 cm, a thickness of about 600 μm, was then produced.

2.3. Materials characterization

X-ray diffraction (XRD) patterns were collected with a Philips X′Pert Pro diffractometer equipped with a primary monochromator (Cu Kα radiation) and a Philips X′Celerator detector for the structural characterization of the specimens. The scans were performed in the 2θ range 20–90° at the scanning speed of 4° min^{-1}. Further XRD studies were also carried out to investigate the chemical compatibility of LSGM with LSCM material. Powder mixture of LSGM with LSCM, in a 1:1 (wt.%) ratio, were ground in an agate mortar and fired at several temperatures for 10 h. Field emission scanning electron microscope (FE-SEM) images of the interface layer LSCM/LSGM before and after SOFC single cell operation were analyzed using a microscope (FE-SEM, PHILIPS 515, Holland) equipped with an X-ray analyzer for energy-dispersive X-ray spectroscopy (EDS).

Simultaneous thermogravimetric-differential thermal analysis (TGA/DTA, Netzsch STA 409) were carried out in static air at heating/cooling rate of 10 °C min^{-1}, to determine the stoichiometry of the nitrates used in the synthesis and to estimate the optimal crystallization temperature of the precursor powders obtained by combustion synthesis technique.

2.4. Characterization of single cell performance

Single cell tests were carried out on a three-electrode arrangement using 20 mm diameter LSGM pellets (600um thick) as electrolyte, $(Pr_{0.7}Ca_{0.3})_{0.9}MnO_3$ (PCM) as cathode material, and LSCM as anode material. The anode was prepared by coating a layer of LSCM slurry, using PVB as binder, onto the electrolyte by screen-printing method and then firing at 1200 °C for 3 h in air. PCM was painted onto the other side (surface of π (0.7 cm)^2 = 1.5386 cm^2) of LSGM as counter-electrode and fired at 1200 °C for 3 h. Experimental techniques, apparatus and the electrochemical cell assembly for SOFC tests have been described previously [23]. A Pt mesh and lead wire were attached to the surface of the cathode using a Pt ink, followed by sintered at 950 °C for 0.5 h. On the anode side, a Au mesh and lead wire were used as the current collector and were attached using a Au ink applied to the edges of the Au mesh, followed by sintering at 850 °C for 0.5 h. The anode side of the structure was then attached to an alumina tube using Au ink and the edges were sealed using a ceramic adhesive. All the anodes were evaluated with the same testing procedure. Hydrogen or gasified ethanol–water mixture (with volume ratio 2:1) were used as fuel and oxygen was used as oxidant. The fuel and oxidant flow rate were all controlled at 25 mL min^{-1}, and the liquid fuel was vaporized by water bath (70 °C) and then brought into the anode surface by nitrogen. The current–voltage curves and electrochemical impedance spectroscopy (EIS) were obtained using an Electrochemical Workstation IM6e (Zahner, GmbH, Germany). These measurements were started after stabilized under a constant discharge voltage of 0.7 V for 4 h in order to obtain a sufficiently stabilized system necessary for a cell testing experiment. Then the current was switched off and the impedance spectra of the electrochemical cell were recorded under open circuit from time to time with amplitude of 20 mV over the frequency range 0.02 Hz to 100 KHz. The measurement was carried out in the temperature range of 700–850 °C in steps of 50 °C. The ohmic resistance of the electrolyte, the cathode and the anode (R_Ω) was estimated from the high frequency intercept of the impedance curves and the overall electrode polarization (interface) resistance (R_E) was directly measured from the differences between the low and high frequency intercepts on the impedance curves.

3. Results and discussion

3.1. Powder characterization

Fig. 1 shows the TGA–DTA curves of the $La_{0.75}Sr_{0.25}Cr_{0.5}Mn_{0.5}O_{3-\delta}$ perovskite gel precursor dried at 383 K. The total weight loss from room temperature to 1250 °C was

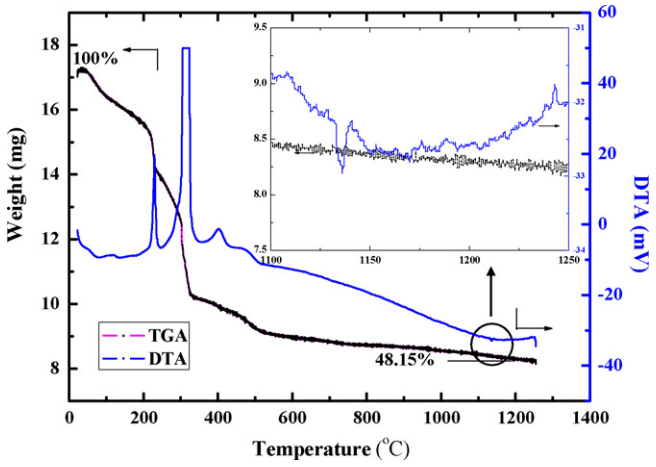

Fig. 1. TGA/DTA curves of the $La_{0.75}Sr_{0.25}Cr_{0.5}Mn_{0.5}O_{3-\delta}$ perovskite gel precursor dried at 110 °C.

51.85 wt.%. A weight loss of about 40 wt.% was observed between 300 and 350 °C, accompanied by two sharp exothermic peaks, which can be attributed to the decomposition of the precursor (exothermic and endothermic processes) and subsequent combustion of organic components (exothermic processes). Between 400 and 700 °C, a further weight loss accompanied by small exothermic effects was observed, also due to combustion of organic residues. The TGA curve showed an additional weight loss of about 1.8 wt.% accompanied by an endothermic peak with its maximum at about 1130 °C (Fig. 1, inset). The weight remained constant above 1150 °C.

To clarify the thermal effects observed above 300 °C, a sample of the $La_{0.75}Sr_{0.25}Cr_{0.5}Mn_{0.5}O_{3-\delta}$ perovskite precursor gel dried at 110 °C was fired at 300 °C for 3 h. Fig. 2 shows the TGA–DTA curves of the sample. In this case, the total weight loss from room temperature to 1250 °C was approximately 20.68 wt.%. A weight loss of about 2.5 wt.% was observed at the vicinity of 300 °C, which can be attributed to the reaction between the residual nitrate and citric acid after the decomposition of the precursor and subsequent combustion of organic components. The exothermic combustion in the air of the

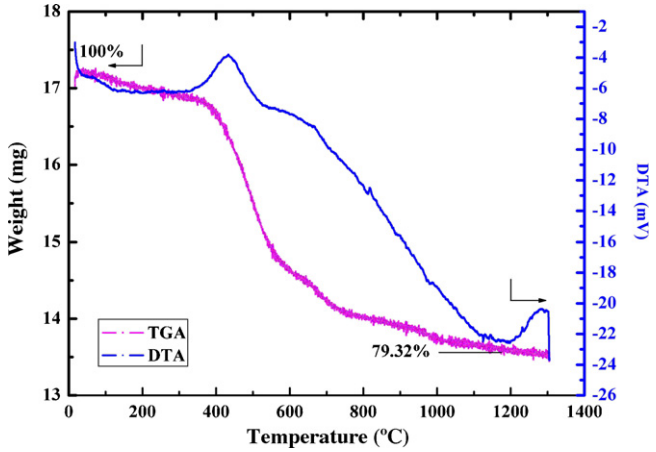

Fig. 2. TGA/DTA curves of the $La_{0.75}Sr_{0.25}Cr_{0.5}Mn_{0.5}O_{3-\delta}$ perovskite precursor dried at 110 °C and then fired at 300 °C for 2 h.

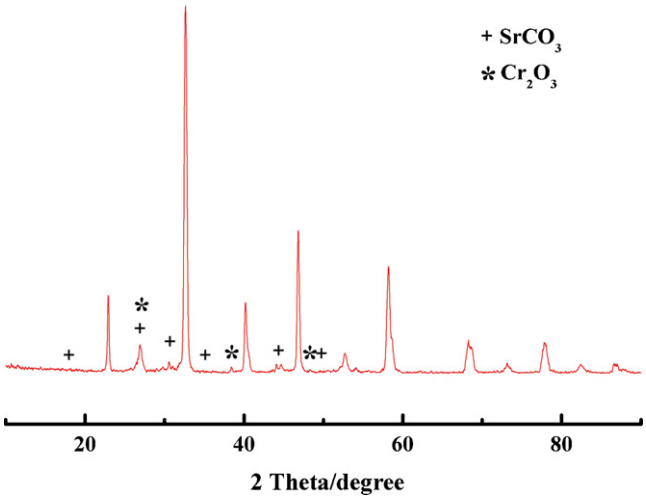

Fig. 3. X-ray diffraction patterns of the perovskite powder calcined at 1000 °C for 2 h. The unmarked peaks correspond to the $La_{0.75}Sr_{0.25}Cr_{0.5}Mn_{0.5}O_{3-\delta}$ structure.

dried polyester showed a weight loss steps, accompanied by an exothermic peak with its maximum at 450 °C. A weight loss of 1.0 wt.% was observed in the temperature range 1140–1160 °C, accompanied by a small endothermic peak with its minimum at 1140 °C, showing that the decomposition process occurs in a step. No weight loss was observed above 1160 °C.

X-ray diffraction (XRD) analysis was performed to elucidate the endothermic decomposition process at about 1150 °C. Fig. 3 shows the XRD pattern of the $La_{0.75}Sr_{0.25}Cr_{0.5}Mn_{0.5}O_{3-\delta}$ powder calcined at 1000 °C for 2 h. Apart from the peaks of the $La_{0.75}Sr_{0.25}Cr_{0.5}Mn_{0.5}O_{3-\delta}$ perovskite-type structures, $SrCO_3$ and Cr_2O_3 phases were detected as impurities.

Fig. 4 shows the XRD pattern of the $La_{0.75}Sr_{0.25}Cr_{0.5}Mn_{0.5}O_{3-\delta}$ powder calcined at 1200 °C for 2 h. The thermal treatment at 1200 °C left only the Cr_2O_3 phase detectable as an impurity. The patterns are identical to the $La_{0.75}Sr_{0.25}Cr_{0.5}Mn_{0.5}O_{3-\delta}$

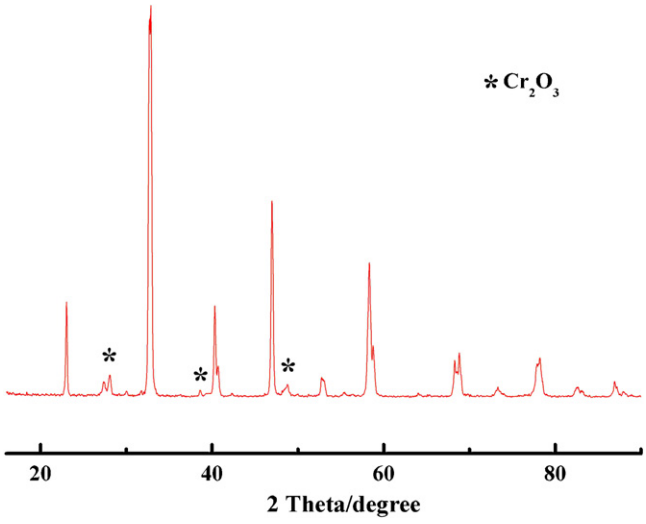

Fig. 4. X-ray diffraction patterns of the perovskite powder calcined at 1200 °C for 2 h. The unmarked peaks correspond to the $La_{0.75}Sr_{0.25}Cr_{0.5}Mn_{0.5}O_{3-\delta}$ structure.

powder obtained at 1400 °C [21], indicating the formation of the perovskite phase of the LSCM powder. Therefore, the endothermic weight loss should be ascribed to the complete decomposition of $SrCO_3$. The presence of a small amount of $SrCO_3$ in the perovskite-type oxide powders calcined at 1000 °C should be due to the reaction between SrO, formed from the nitrate decomposition, and CO_2, produced from combustion processes. The nitrate–citrate processes can also lead to the presence of residual carbon after the precursor decomposition/oxidation [24]. Giving the combined results of TGA–DTA and XRD analyses, showing that the powder calcined at 1200 °C was made nearly entirely of LSCM single-phase, the films for electrochemical characterization were prepared by screen-printing the LSCM powder calcined at 1200 °C on the side of the tape cast LSGM.

3.2. Chemical compatibility study

The XRD patterns of the binary-mixed-systems LSGM/LSCM and LSGM/PCM at different temperature are shown in Figs. 5 and 6. No additional diffraction peaks were found after firing mixtures of LSGM/LSCM and LSGM/PCM in the air for 5 h, between room temperature and 1200 °C indicating a good chemical compatibility at intermediate temperature (≤800 °C). Nevertheless, certain reactivity could be observed between LSGM and LSCM above 1300 °C, between LSGM and PCM at 1250 °C. No reaction was observed for the LSGM/LSCM system at 1000–1200 °C. Du and Sammes [25] reported that no interactions were detected from XRD data in their experiments of fabrication of bilayer samples of LSGM and LSCM at 1500 °C for 2 h. However, they found severe reactions in samples after 6 h and over at 1500 °C, forming low conductive phases. They used energy-dispersive spectrometry (EDS) analysis to find reaction-diffusion zones in the range 50–150 μm. Nevertheless, they indicate from their overall results that LSCM is a thermomechanically and chemically compatible anode material with LSGM electrolyte at the fuel cell operating temperatures and fuel cell fabrication conditions (at 1500 °C for 2 h). In this work, LSCM material had been applied to the electrolyte LSGM at 1200 °C for 3 h, and LSGM and LSCM did not show apparently remarkable signs of reaction in fired compacted powder. These results indicate that LSCM is a thermomechanically and chemically compatible anode material with LSGM electrolyte at the fuel cell operating temperatures and fuel cell fabrication conditions (at 1200 °C for 3 h). However, the XRD pattern of the mixture LSGM/LSCM at 1300 °C for 3 h (Fig. 5(g)) showed a reaction which becomes stronger at 1400 °C (Fig. 5(h)). The interaction between LSGM/LSCM has not been studied further and more studies are necessary. In the PCM/LSGM case, the PCM cathode material fired at 1200 °C onto LSGM did not show obvious signs of reaction.

3.3. Fuel cell tests

3.3.1. Current–voltage measurements

Fig. 7 shows typical voltage and power density versus current density for a SOFC with the electrolyte-supported system LSCM/LSGM/PCM while running on humidified hydrogen

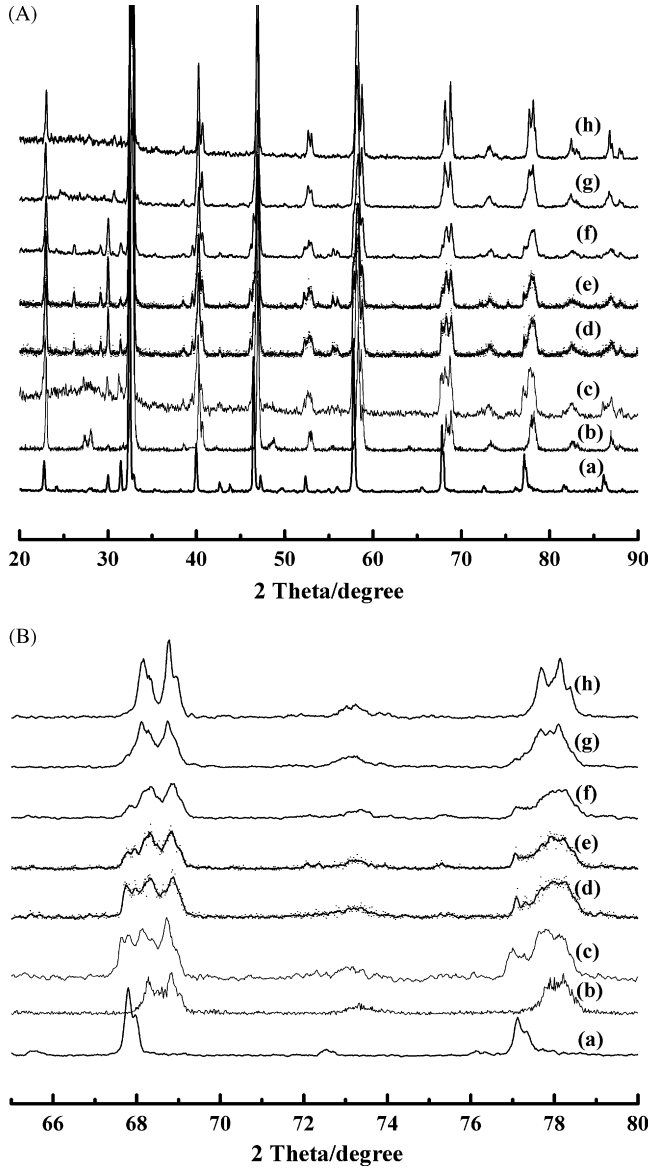

Fig. 5. XRD patterns of LSGM (a), LSCM (b), and LSGM + LSCM at the following temperatures: room temperature (c), 1000 °C (d), 1100 °C (e), 1200 °C (f), 1300 °C (g), 1400 °C (h) (A) and magnification in the 2θ range 65–80° (B).

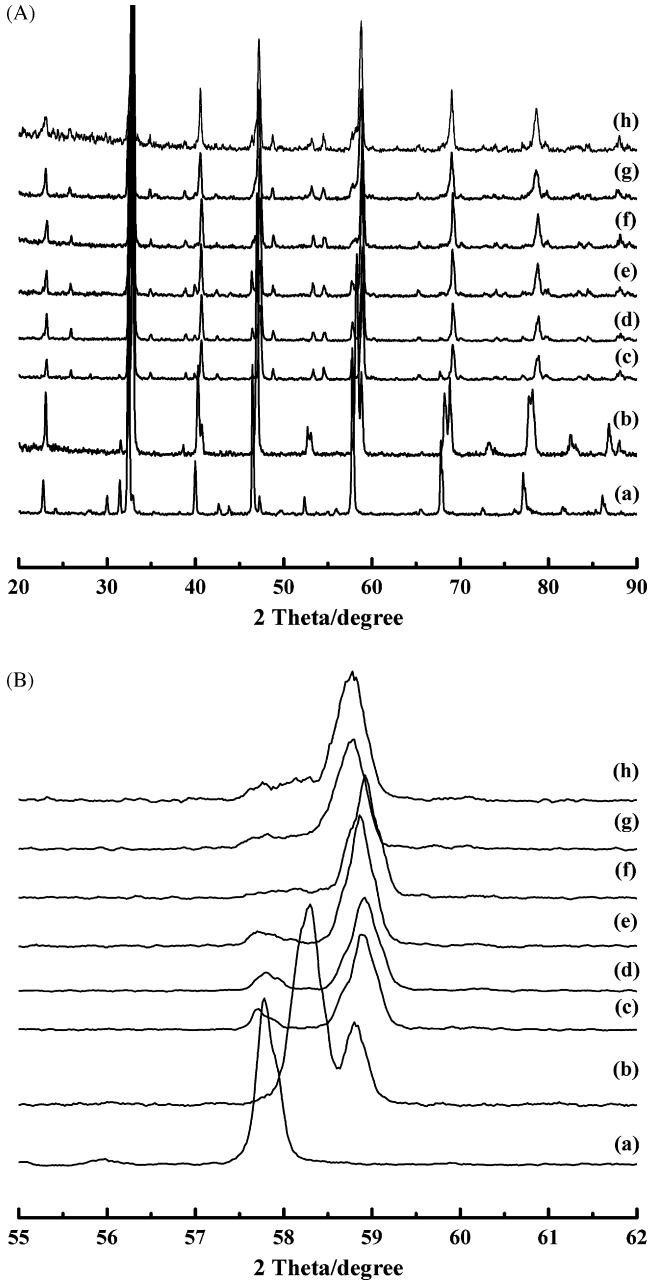

Fig. 6. XRD patterns of LSGM (a), PCM (b), and LSGM + PCM at the following temperatures: room temperature (c), 1100 °C (d), 1200 °C (e), 1250 °C (f), 1300 °C (g), 1400 °C (h) (A) and magnification in the 2θ range 65–80° (B).

(a) and ethanol stream (b) at 850, 800 and 750 °C, respectively. We could see that the open circuit voltages (OCV) for H_2 and C_2H_5OH stream were, respectively, 1.146–1.165 and 1.176–1.164 V in the temperature range. It revealed that LSGM electrolyte was dense enough that resulted in higher values of OCV. The performance of the cell while operating on humidified hydrogen was modest with a maximum power density of 165, 99 and 62 mW cm^{-2} at 850, 800 and 750 °C, respectively. The highest power density of the cell while operating on ethanol stream was 160, 101 and 58 mW cm^{-2} at 850, 800 and 750 °C, respectively, which were lower than those on hydrogen. Taking into consideration the thickness of the LSGM electrolyte (600 μm) and the LSCM anode (65 μm), we have obtained feasible performance about the electrolyte-supported system LSCM/LSGM/PCM while running on humidified hydrogen and ethanol stream at different temperature. Next work is to decrease the thickness of the LSGM electrolyte and the LSCM anode in order to improve the cell performance.

A detailed study of cells running on hydrogen has shown that cell power densities can be limited by a number of factors, including concentration polarization [26,27]. The decrease in cell power density for ethanol stream relative to hydrogen may be related to the higher mass of ethanol molecules, which yields slower gas-phase diffusion and increased concentration polarization. However, it is also noted that each ethanol molecule reacts with six times as many oxygen ions as each hydrogen molecule, so less ethanol gas-phase diffusion is needed to yield the same cell current density. Another possible explanation is the

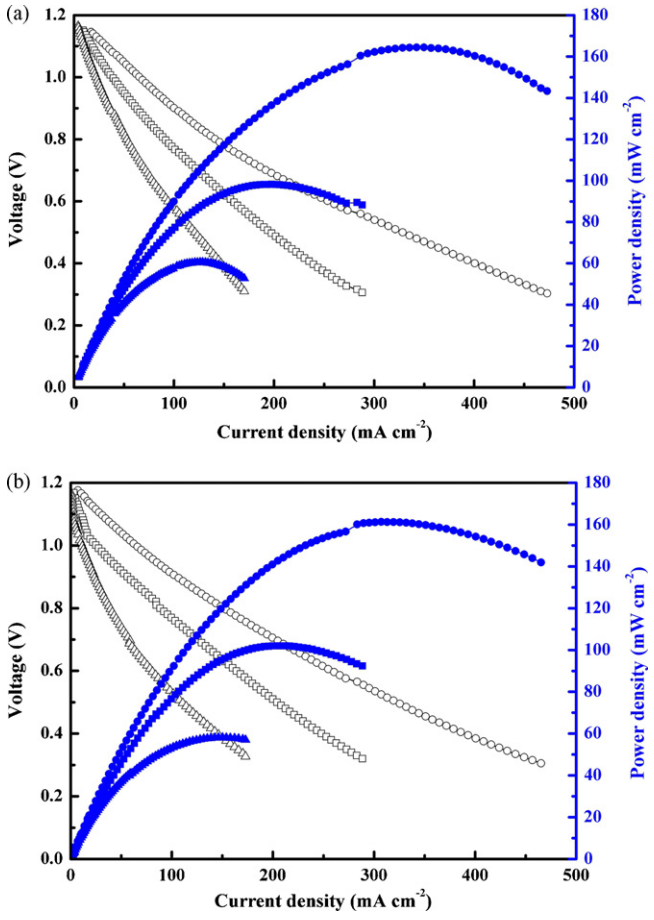

Fig. 7. Voltage and power density vs. current density for a SOFC with the electrolyte-supported system LSCM/LSGM/PCM at different temperature using humidified hydrogen (a) or ethanol stream (b) as fuel and oxygen as oxidant: (◯, ●) 850 °C; (□, ■) 800 °C; (△, ▲) 750 °C.

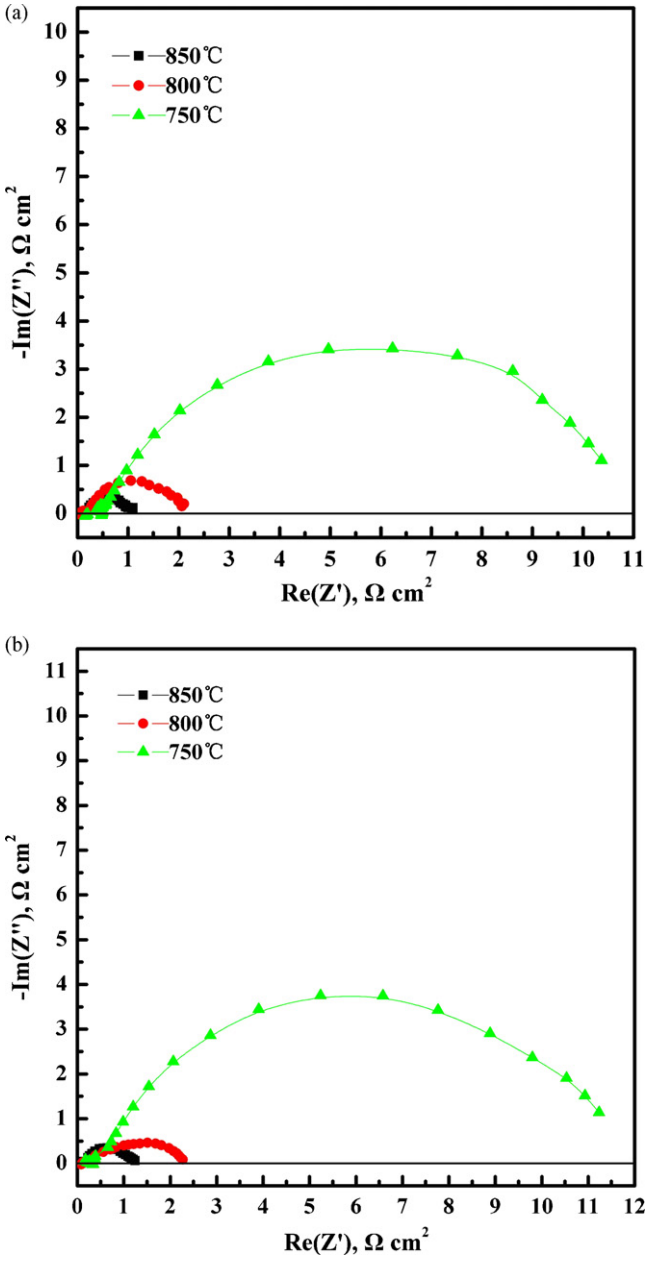

Fig. 8. Electrochemical impedance spectra for a SOFC with the electrolyte-supported system LSCM/LSGM/PCM at different temperature using humidified hydrogen (a) or ethanol stream (b) as fuel and oxygen as oxidant under open circuit.

difference in the nature of the oxidizing and reducing species, which makes the charge transfer in ethanol more complex and difficult. H_2 is obviously more active and more effective for reduction. C_2H_5OH is much less reactive than H_2 in heterogeneous oxidation, thus resulting in a higher polarization resistance associated with slower electrochemical oxidation of ethanol versus hydrogen. Therefore, more work is required to do to study the steps and mechanism of ethanol oxidation by analyzing the components of the fuel effluent and improve performance of the cell running on ethanol fuel.

3.3.2. *Electrochemical impedance spectroscopy (EIS) study*

Fig. 8 shows a comparison of typical EIS results, from cell with the electrolyte-supported system LSCM/LSGM/PCM while running on humidified hydrogen (a) and ethanol stream (b) under open circuit at different temperature, respectively, associated with the *V–I* curves in Fig. 7. As could be expected through examination of Fig. 8, the cell exhibits less total impedance ($R_\Omega + R_E$) in humidified hydrogen than that in ethanol stream at different temperature, which is in good agreement with the results shown in Fig. 7.

Attending to the microstructure, Fig. 9 shows the FE-SEM micrograph of the LSCM thick film (65 μm) sintered at 1200 °C for 3 h. The microstructure obtained is very promising, a highly porous structure made of sintered perovskite-structure particles. Fig. 10 shows the FE-SEM micrograph of the interface LSGM/LSCM after fuel cell test in ethanol steam at 750 °C for 60 h. In general, the distribution of the grains in the anode material is fairly homogeneous with an average grain size of 2 μm. Moreover, the loss of adherence and partial grain agglomeration of LSCM material after fuel cell test shown in Fig. 10, is possibly other reasons for the lower electrochemical performance respect LSCM material-based systems. In addition, further work will be done to reduce the thickness of LSCM anode film and electrolyte layer with a view to achieving comparable perfor-

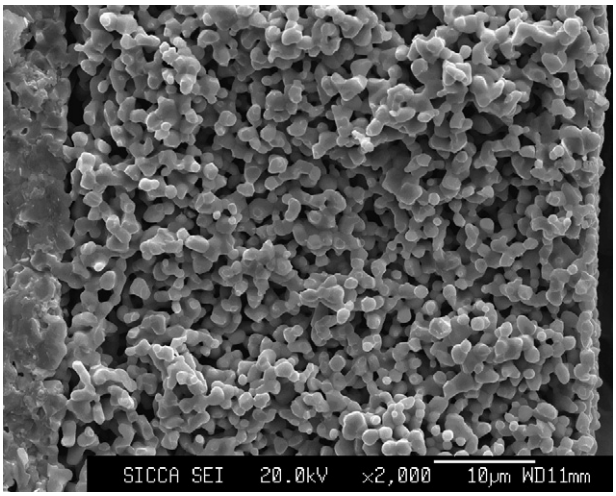

Fig. 9. FE-SEM micrograph of the LSCM thick film sintered at 1200 °C for 3 h.

mances of the electrolyte-supported cell LSCM/LSGM/PCM running on ethanol stream at 750 °C.

3.4. Cell stability tests

The stabilization and degradation of the electrolyte-supported cell LSCM/LSGM/PCM were also investigated in ethanol stream at 750 °C during the measurements. We recorded the curve of power density as a function of time for the cell operating on ethanol steam at 750 °C, shown in Fig. 11. We can find that the performance of the cell almost kept constant with a little augment of power density with time in the period of 60 h. In one case, the cell was operated for >60 h in ethanol stream at 750 °C, before the test was stopped with the cell still running well. Very little carbon was detected on the anodes, suggesting that carbon deposition was limited during cell operation. More work is required to do to provide meaningful information about the stability of the anode component in the long run.

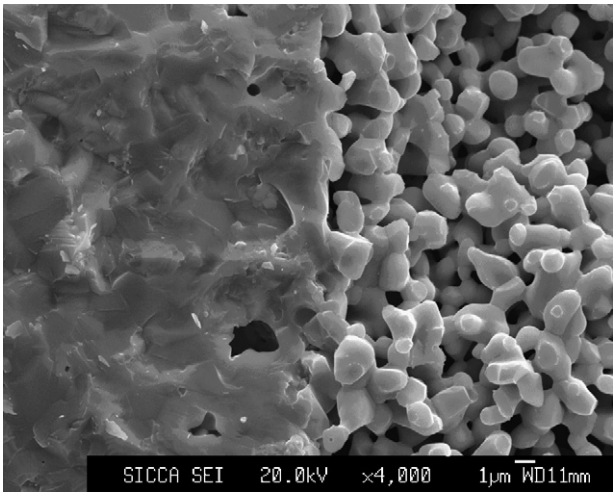

Fig. 10. FE-SEM micrograph of the interface LSGM/LSCM after fuel cell test in ethanol steam at 750 °C for 60 h.

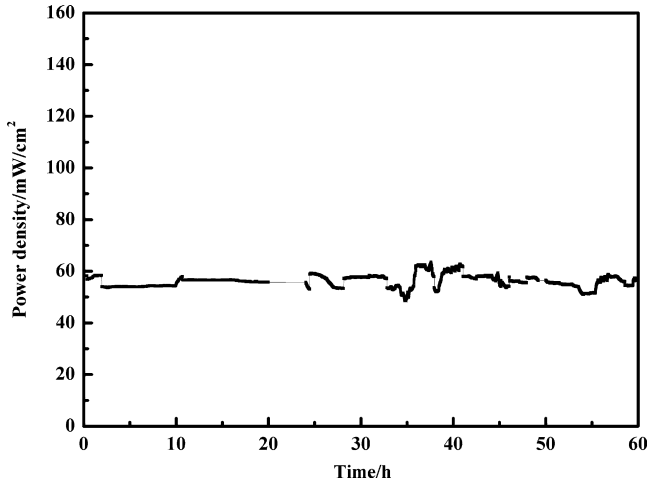

Fig. 11. Power density of a SOFC with the electrolyte-supported system LSCM/LSGM/PCM using ethanol stream as fuel and oxygen as oxidant at 750 °C during the aging process.

4. Conclusions

Perovskite-structure $La_{0.75}Sr_{0.25}Cr_{0.5}Mn_{0.5}O_{3-\delta}$ (LSCM) powders were prepared using a simple combustion process. For the electrochemical characterization of fuel cell, $La_{0.8}Sr_{0.2}Ga_{0.8}Mg_{0.2}O_3$ (LSGM) was used as electrolyte and $(Pr_{0.7}Ca_{0.3})_{0.9}MnO_3$ (PCM) and $La_{0.75}Sr_{0.25}Cr_{0.5}Mn_{0.5}O_{3-\delta}$ (LSCM) as cathode and anode material, respectively. Fuel cell tests were carried out using humidified hydrogen or ethanol stream as fuel and oxygen as oxidant. The performance of the conventional electrolyte-supported cell LSCM/LSGM/PCM while operating on humidified hydrogen was modest with a maximum power density of 165, 99 and 62 mW cm^{-2} at 850, 800 and 750 °C, respectively, the corresponding values for the cell while operating on ethanol stream was 160, 101 and 58 mW cm^{-2}, respectively. Cell stability tests indicated no significant degradation in performance had been observed after 60 h of cell testing when LSCM anode was exposed to ethanol steam at 750 °C, suggesting that carbon deposition was limited during cell operation.

Acknowledgements

The authors thank the Shanghai Institute of Ceramics Chinese Academy of Sciences, the Postdoctoral Foundation of Shanghai (Grant No. 06R214156) and the Postdoctoral Foundation of China (2006) for the grants that support this research.

References

[1] B.C.H. Steele, A. Heinzel, Nature 414 (2001) 345–352.
[2] C. Lu, W.L. Worrell, C. Wang, S. Park, H. Kim, J.M. Vohs, R.J. Gorte, Solid State Ionics 152–153 (2002) 393.
[3] J. Liu, S.A. Barnett, Solid State Ionics 158 (2003) 11.
[4] J.-H. Koh, Y.-S. Yoo, J.-W. Park, H.C. Lim, Solid State Ionics 149 (2002) 157.
[5] J.B. Wang, J.-C. Jang, T.-J. Huang, J. Power Sources 122 (2003) 122.
[6] C.H. Bartholomew, Catal. Rev. Sci. Eng. 24 (1982) 67.
[7] R.T.K. Baker, Carbon 27 (1989) 315.
[8] B.C.H. Steele, Solid State Ionics 86–88 (1996) 1223.

[9] K. Hernadi, A. Fonseca, J.B. Nagy, A. Siska, I. Kiricsi, Appl. Catal. A 199 (2000) 245.
[10] J.H. Koh, Y.-S. Yoo, J.-W. Park, H.C. Lim, Solid State Ionics 149 (2002) 157.
[11] T. Ishihara, H. Matsuda, Y. Takita, J. Am. Chem. Soc. 116 (1994) 3801.
[12] S. Kim, M.C. Chun, K.T. Lee, H.L. Lee, J. Power Sources 93 (2001) 279.
[13] I.N. Sora, R. Pelosato, G. Dotelli, C. Schmid, R. Ruffo, C.M. Mari, Solid State Ionics 176 (2005) 81.
[14] T. Ishihara, J.A. Kilner, M. Honda, N. Sakai, H. Yokokawa, Y. Takita, Solid State Ionics 113–115 (1998) 593.
[15] J.B. Goodenough, Nature 404 (2000) 821.
[16] M. Mori, Y. Hier, J. Am. Ceram. Soc. 84 (2001) 2573.
[17] J. Vulliet, B. Morel, J. Laurencin, G. Gauthier, L. Bianchi, S. Giraud, J.Y. Henry, F. Lefebvre-Joud, S.C. Singhal, M. Dokiya (Eds.), SOFC-VIII, vol. 2003-07, The Electrochem. Soc., Pennington, NJ, 2003, p. 803.
[18] J. Sfeir, P.A. Buffat, P. Mockli, N. Xanthopoulos, R. Vasquez, H.J. Mathieu, J. Van herle, K.P. Thampi, J. Catal. 202 (2001) 229.
[19] J. Sfeir, J. Power Sources 118 (2003) 276.
[20] S. Tao, J.T.S. Irvine, Nat. Mater. 2 (2003) 320.
[21] S. Tao, J.T.S. Irvine, J. Electrochem. Soc. 151 (2004) A252.
[22] S. Jain, K. Adiga, V. Vrneker, Combust. Flame 40 (1981) 71.
[23] X.-F. Ye, et al., J. Power Sources 164 (2007) 203.
[24] M.S.G. Baythoun, F.R. Sale, J. Mater. Sci. 17 (1982) 2757.
[25] Y. Du, N.M. Sammes, Proceedings of the 9th International Symposium on Solid Oxide Fuel Cells (SOFC-IX), PV 2005-07, The Electrochemical Society, 2005, p. 1127, ISBN: 1-56677-465-9.
[26] S. de Souza, S.J. Visco, L.C. De Jonghe, J. Electrochem. Soc. 144 (1997) L35–L37.
[27] J.W. Kim, A.V. Virkar, K.Z. Fung, K. Mehta, S.C. Singhal, J. Electrochem. Soc. 146 (1) (1999) 69–78.